

CINTAL - Centro de Investigação Tecnológica do Algarve
Universidade do Algarve

Tomografia Passiva Costeira
(TOMPACO)

Inversion results with active data - Phase 2
(Part II)

S.M. Jesus and C. Soares

Rep 06/01 - SiPLAB
26/Dec/2001

University of Algarve
Campus da Penha
8000, Faro,
Portugal

tel: +351-289800131
fax: +351-289864258
cintal@ualg.pt
www.ualg.pt/cintal

Work requested by	CINTAL Universidade do Algarve, Campus da Penha, 8000 Faro, Portugal tel: +351-289800131, cintal@ualg.pt, www.ualg.pt/cintal
Laboratory performing the work	SiPLAB - Signal Processing Laboratory Universidade do Algarve, FCT, Campus de Gambelas, 8000 Faro, Portugal tel: +351-289800949, info@siplab.uceh.ualg.pt, www.ualg.pt/uceh/adeec/siplab
Projects Title	TOMPACO - CNR, Italy TOMografia PAssiva COstiera - (Phase 2 - Part II)
Authors	S.M.Jesus and C.Soares
Date	Dec 26, 2001
Reference	06/01 - SiPLAB
Number of pages	31 (thirty one)
Abstract	This report shows the acoustic inversion results obtained on the INTIFANTE'00 data set, Events II and V.
Clearance level	UNCLASSIFIED
Distribution list	DUNE (1), ENEA (1), IH (1), SiPLAB (1), CINTAL (1)
Total number of copies	5 (five)

Copyright Cintal@2001

Foreword and Acknowledgment

This report presents the inversion results obtained so far on the data set acquired during Events II and V of the INTIFANTE'00 sea trial. The INTIFANTE'00 sea trial took place off the Tróia Peninsula, near Setúbal, approximately 50 km south of Lisbon, Portugal, during the period 9 - 29 October 2000.

The institutions responsible for the sea trial are:

- Instituto Hidrográfico, Rua das Trinas 49, Lisboa, Portugal.
- CINTAL, Universidade do Algarve, Faro, Portugal.
- ISR, Instituto Superior Técnico, Lisboa, Portugal.

Other institutions involved are:

- Ente Nazionale per l'Energia ed l'Ambiente, La Spezia, Itália

The INTIFANTE organizers would like to thank:

- the crew of the research vessel NRP D. Carlos I
- the NATO SACLANT Undersea Research Centre for lending the acoustic sound source and power amplifier.
- Enrico Muzi, from SACLANTCEN, for his participation in the acoustic source preparation and testing.

intentionally blank

Contents

List of Figures	VII
1 Introduction	9
2 The forward problem	11
2.1 Generalities	11
2.2 The baseline model	13
2.3 Ocean sound speed modelling	15
3 The inverse problem	17
3.1 Focalization: a method for global inversion	17
3.2 GA Optimization	18
3.3 Event II: moving source inversion in a range-independent environment . . .	18
3.4 Event V - range independent, PRN stationary source	22
3.5 Event V - range dependent, PRN moving source	26
4 Conclusion	29

intentionally blank

List of Figures

2.1	<i>INTIFANTE'00 bathymetry for events II, IV, V and VI.</i>	12
2.2	<i>Environmental model for the propagation scenario along the NE leg.</i>	12
2.3	<i>Transmission loss along the NE leg with CSNAP model at: 150 Hz (a), 300 Hz (b), 500 Hz (c) and 800 Hz (d).</i>	13
2.4	<i>Transmission loss along the NE leg with RAM model at: 150 Hz (a), 300 Hz (b), 500 Hz (c) and 800 Hz (d).</i>	14
2.5	<i>Baseline environmental model for the range-independent propagation scenario.</i>	14
2.6	<i>XBT based data used for ocean sound speed estimation: mean sound speed profile (a) and empirical orthonormal functions (EOFs) (b).</i>	16
3.1	<i>Event II: bathymetry and ship course along NW leg.</i>	18
3.2	<i>Event II: source ship speed and heading along NW leg.</i>	19
3.3	<i>Event II: source - VLA range as estimated from GPS data.</i>	19
3.4	<i>Tomography results for ocean sound speed during moving source portion of Event 2: time series of sound speed profiles (a) and depth - time plot of inverted sound speed (b).</i>	20
3.5	<i>Focalization results for Event 2: Bartlett power (a), source range (b), source depth (c), receiver depth (d), sediment compressional speed (e), sediment thickness (f), sub-bottom compressional speed (g), VLA tilt (h), EOF coefficient 1 (i), EOF coefficient 2 (j).</i>	21
3.6	<i>Comparison of the VLA received acoustic pressure with the CSNAP prediction using the baseline model and the model after focalization at frequencies of: 300 Hz (a) and 500 Hz (b).</i>	22
3.7	<i>Event V: bathymetry and ship course along NE leg.</i>	23
3.8	<i>Event V: source ship speed and heading along NE leg.</i>	23
3.9	<i>Event V: source - VLA range as estimated from GPS data.</i>	24
3.10	<i>Tomography results for ocean sound speed during arc shaped moving source portion of Event 5: time series of sound speed profiles (a) and depth - time plot of inverted sound speed (b).</i>	24

3.11	<i>Focalization results for arc shaped portion of Event 5: Bartlett power (a), source range (b), source depth (c), receiver depth (d), sediment compressional speed (e), sediment thickness (f), sub-bottom compressional speed (g), VLA tilt (h), EOF coefficient 1 (i), EOF coefficient 2 (j).</i>	25
3.12	<i>Baseline environmental model for the range-dependent propagation scenario of Event 5.</i>	26
3.13	<i>Tomography results for ocean sound speed during range-dependent moving source portion of Event 5: time series of sound speed profiles (a) and depth - time plot of inverted sound speed (b).</i>	27
3.14	<i>Focalization results for range-dependent portion of Event 5: Bartlett power (a), source range (b), source depth (c), receiver depth (d), sediment compressional speed (e), sediment thickness (f), sub-bottom compressional speed (g), VLA tilt (h), EOF coefficient 1 (i), EOF coefficient 2 (j).</i>	28

Chapter 1

Introduction

Ocean Acoustic Tomography (OAT) is nowadays a widely accepted technique for ocean probing by acoustic means. The principle of determining environmental properties from acoustic signal perturbations is highly dependent on the capacity of predicting sound propagation between source and receiver. In water depths greater than, say, 1000 m and at useful frequencies, sound waves behave much like in free space and are therefore mostly influenced by water column density scattering. In coastal waters, depths vary between 0 and 500 m which make sound behave much more like trapped waves. In that case sea bottom and sea surface properties become predominant, leading to a decrease of the influence of water column properties on sound prediction at useful ranges. As a consequence, shallow water tomography becomes a difficult task when bottom properties are unknown or poorly known. Along the same lines, sea surface and sea bottom sound interaction in shallow water leads to a strong dependence of sound prediction on ocean bathymetry along the direction of propagation. Similarly, and as in classical deep water OAT, sound prediction in shallow water is strongly dependent on source-receiver geometry.

A basic principle in OAT is that in order to extract water column information from the acoustic data, all the other geometrical and environmental properties are known to a degree of precision sufficient to allow accurate sound prediction to discriminate the variation of the required parameters. Classical ocean tomography assumes that there is a full control both on the source and receiver positions. In shallow water the knowledge of source-receiver relative position along time would lead to the necessity to know the bathymetry and bottom properties along the propagation path at all times. In the case where the receiver is a vertical line array (VLA) and the source is moving, that requires the knowledge of bathymetry and bottom properties in a vast area around the VLA location.

The main objective of the TOMPACO¹ project is to relax the need for the active sound source to illuminate the environment. Active sources are in that case replaced by sources of opportunity as passing by ships or natural sound sources. Passing from active to passive sources adds several difficulties to the problem: the source emitted waveform becomes unknown and uncontrollable, the source position is unknown and as a consequence bathymetry and bottom properties become also unknown. In other words, for practical purposes, passing from active to passive shallow water tomography is equivalent to passing from a “simple” inversion of the water column properties to a full inversion of source position, bottom properties, bathymetry and water column properties. That represents a dramatical increase of the parameter search space with its associated possible non-uniqueness solutions and numerical computation problems.

¹TOMografia PAssiva COstiera - Passive Coastal Tomography

There are several aspects that should be taken into account when attempting to demonstrate shallow water passive tomography: one is that it is, at least at this stage, unrealistic to attempt to perform a full scale inversion test with unknown environmental and source conditions, other is that environmental and geometrical effects should be as much as possible tackled separately. Another important aspect is that care should be taken to isolate cross-effects between parameters in order to obtain absolute water column estimates and another last important aspect is that care should also be taken when combining information across-frequency taking into account that the ultimate goal is to operate with unmanned sound sources that are, by nature, highly non-stationary and with possibly unpredictable phase evolutions along time.

The INTIFANTE'00 sea trial was partially designed to cope with the different situations encountered in passive tomography (see [1, 2] for a complete experiment and data description). The present report attempts to demonstrate the concept of TOMPACO using an active source in a passive shallow water tomography scenario. By this it is meant that an active source is used in a shallow water scenario where hypotheses are progressively relaxed, one at a time, leading to more complex problems that will eventually lead to a full passive tomography approach.

This report is organized as follows: chapter 2 describes the forward problem encountered in the INTIFANTE'00 data set - Events II and V are respectively taken as examples for a known moving source in a range independent environment and an unknown fixed source in a range dependent or independent scenario; chapter 3 approaches the same cases shown in chapter 2 but from the acoustic inverse point of view. Chapter 3 presents the concluding remarks and perspectives for further work.

Chapter 2

The forward problem

2.1 Generalities

The INTIFANTE'00 sea trial was primarily designed for testing acoustic data inversion techniques aiming at estimating water column properties and source position. However, since direct analytical/numerical inversion is in most practical cases not possible, one is limited to repeating forward runs and compare the output to the observed data. Therefore, forward acoustic prediction is of paramount importance in order to obtain stable and accurate inversion results.

The first task is to select a suitable forward model being able to take into account the environmental features of the area and to produce an accurate response in the desired frequency band. As a side requirement, but nonetheless important, the forward model should be fast enough for being able to produce thousands of predictions in a reasonable time. To that end, and when range-dependency is involved in shallow water, coupled mode or parabolic equation based models are the choice. Parabolic equation models are known to be very accurate in range-dependent environments but are also known to be quite slow when broadband calculations are required.

The sea trial site bathymetry for events II, IV, V and VI is shown in figure 2.1. Latitude and longitude are set in military coordinates for continental Portugal in km. The area covered during this events is approximately 11 by 5.5 km along two acoustic transmission legs, termed as NW and NE legs relative to the vertical array (VLA) location marked by a \diamond sign at coordinates 129.981 km longitude West and 148.466 km latitude North. Note that the NE leg is mildly range-dependent between 60 and 120 m depth while the NW leg is approximately range-independent with a depth variation of less than 6 m around a mean depth of 119 m in 6 km length (1.4 m standard deviation).

In order to give an idea of the comparison between parabolic and coupled normal mode, the CSNAP [3] and RAM [4] propagation codes were tested on a range-dependent section along the NE sea trial leg. The environmental model used for these simulations is shown in figure 2.2.

The transmission loss plots obtained at four characteristic frequencies of 150, 300, 500 and 800 Hz with model CSNAP are shown in figure 2.3. Sound interaction with the ocean bottom can easily be seen in this example, specially close to the sound source and at low frequencies. Sound penetration in the sea bottom decreases with increasing frequency as

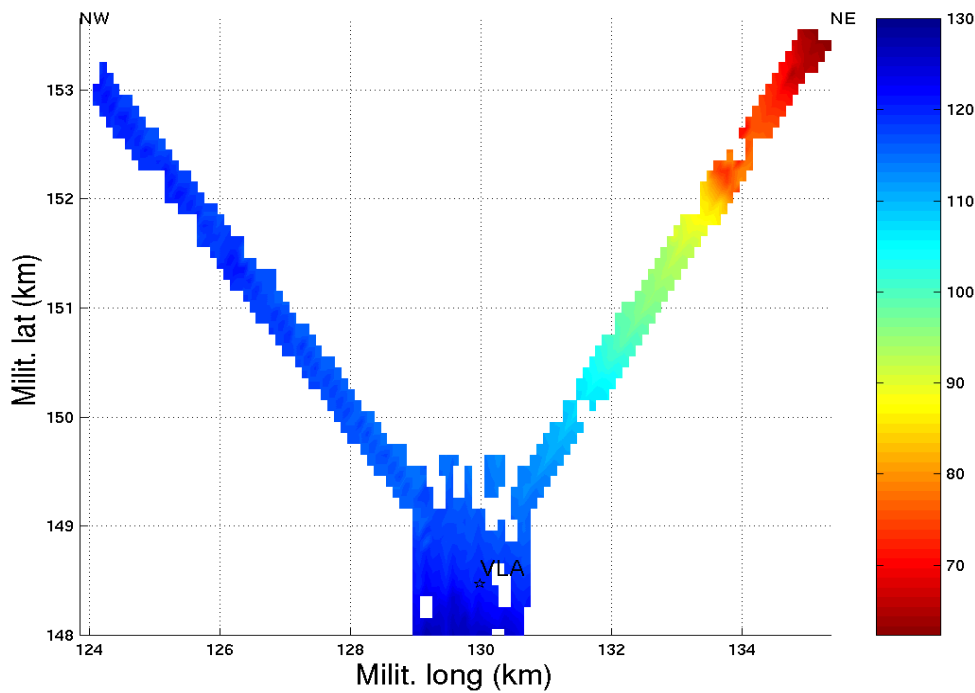


Figure 2.1: *INTIFANTE'00* bathymetry for events *II*, *IV*, *V* and *VI*.

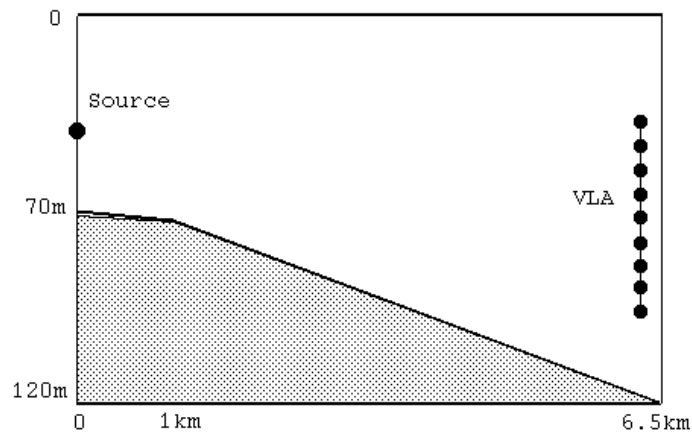


Figure 2.2: *Environmental model for the propagation scenario along the NE leg.*

expected. High sound energy patches at close range tend to fragment also with increasing frequency and the consequent increase in the number of modes. At all frequencies the absolute mean sound power at 6.5 km range is approximately constant.

Similar forward runs have been conducted with the RAM propagation code in the same environment and at the same source frequencies - figure 2.4. Several differences can be noticed: there is a clear difference at very close range regarding the energy level and the energy penetration in the bottom; there is also a mean sound pressure difference of about 7-8 dB over the whole figure. Apart from that, the acoustic power distribution is quite similar for the two models. There are at least two main known differences between these two codes: one is that the parabolic solver is a marching solution that requires an initializer at range $r = 0$ (starter) and thus possible discrepancies at close range; the

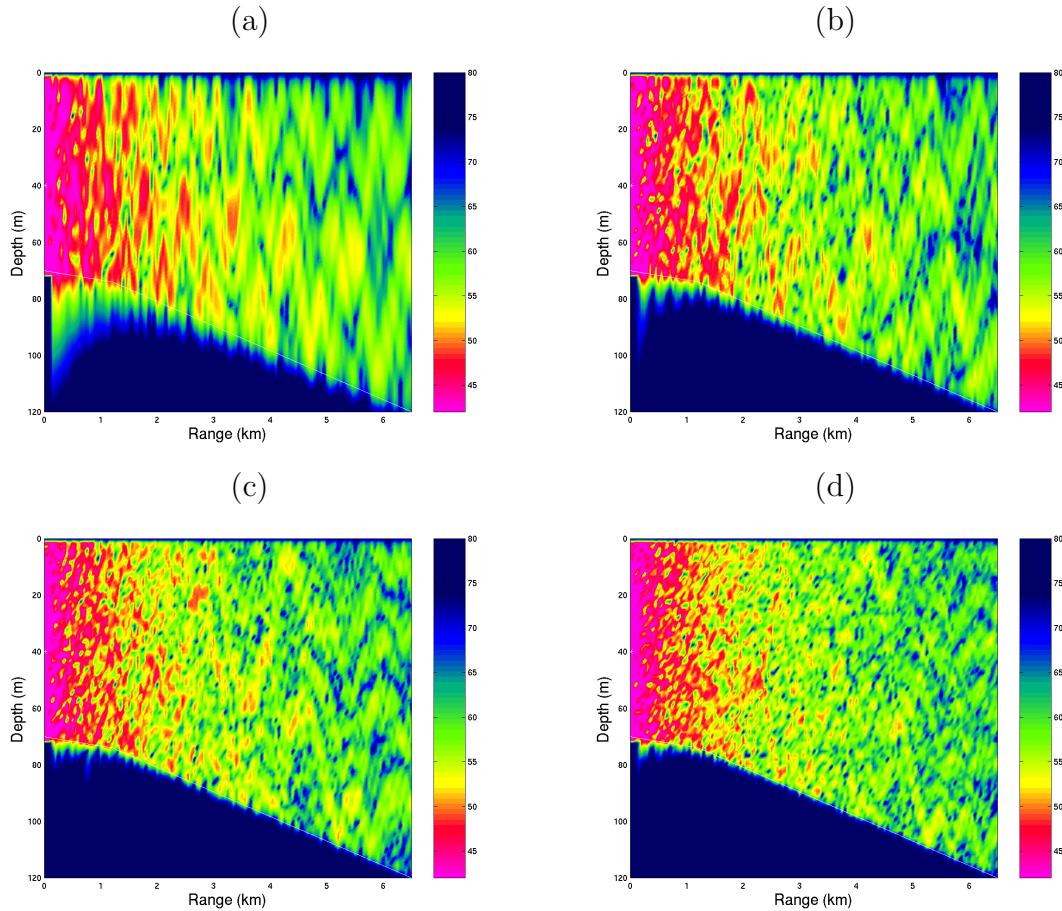


Figure 2.3: *Transmission loss along the NE leg with CSNAP model at: 150 Hz (a), 300 Hz (b), 500 Hz (c) and 800 Hz (d).*

second difference is that the RAM model only takes into account the forward field and not the possible reflections, which may account for a smaller loss than with the normal-mode code CSNAP in this example. These two differences may justify the observed discrepancies between the simulated results.

Although RAM run very fast on our machine and a parallel version is available (RAMP) there is little information on how to create a transfer function output (complex numbers) that is required for matched-field calculations. Finally, since our environmental model is weakly range dependent, 55 m in 6.5 km, a coupled mode solution is known to be sufficiently accurate, and therefore our choice was towards the use of the CSNAP model.

2.2 The baseline model

An important first step in tomographic inversion is the choice of an environmental model able to represent the mean characteristics of the media where the signal is propagating. Such model will be called the baseline model and generally includes all the a priori information available for the problem at hand.

The baseline environmental model consists of an ocean layer overlying a sediment layer and a bottom half space assumed to be range independent, as shown in figure 2.5. For

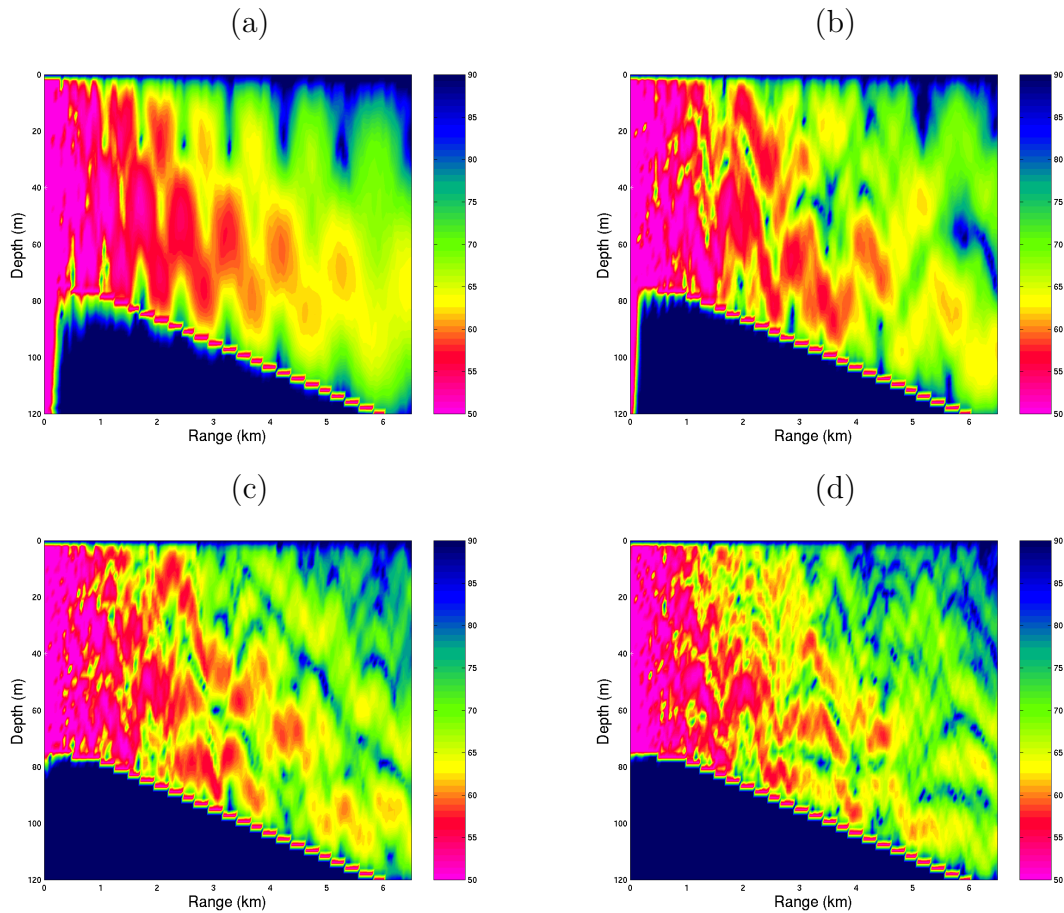


Figure 2.4: Transmission loss along the NE leg with RAM model at: 150 Hz (a), 300 Hz (b), 500 Hz (c) and 800 Hz (d).

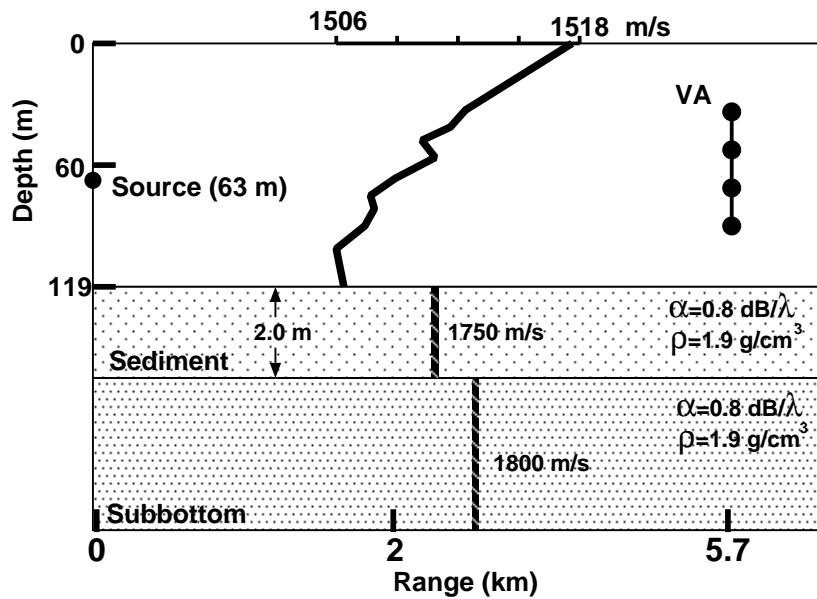


Figure 2.5: Baseline environmental model for the range-independent propagation scenario.

the purpose of inversion the forward model parameters were divided into four parameter subsets: geometric, sediment, bottom, and water sound speed. The geometric parameters

included source range, source depth, receiver depth and bathymetry. The sediment and bottom halfspace are shown in figure 2.5 and are based on vague historical data. The water column sound speed shown is the mean temperature profile measured at the VLA thermistors (see environmental description in [1, 2]).

2.3 Ocean sound speed modelling

Another important problem when inverting acoustic data is the difficulty associated with the representation of the sound speed field in time, depth and range by a finite set of invariant parameters. The solution for this problem is known as data regularization, and it consists on the expansion of the temperature, or equivalently the sound speed, field on a basis of functions representative of the data set to be estimated. Since from that moment on, the inverse problem becomes constrained on the basis of functions used, it is of paramount importance to determine a suitable function basis for each data set. It is well known that regularization is a powerful method that leads to a faster convergence and a higher uniqueness of the optimal solution since the a priori information already contained in the set of basis function allows to start the search closer to the optimal solution than if no such information was available. A well known method for obtaining a suitable basis functions is to calculate the Empirical Orthogonal Functions (EOF) as the eigenfunctions of the data correlation matrix. Assuming that the temperature field is stationary in range, this method requires a time series representative of the data under observation taken in the location and at the time of the experiment. In other words, in order to obtain a tomographic image of the temperature data one needs to already have an observation of that data. In many situations and also on passive tomography that is a strong a priori requirement that is not always fulfilled. Alternatively, it has been shown that a suitable set of eigenfunctions can be formed from the hydrodynamical normal modes (HNM) of oscillation of the temperature field [5]. In that case only a mean temperature profile from archival data is necessary. For the INTIFANTE'00 data set such HNM have been calculated as a requirement for the TOMPACO project - Phase 2[6].

In our case, since a full set of observations were readily available, the EOF method was used for parameterization of the ocean sound speed. Note that a similar expansion could be done using the temperature data as long as the salinity profile is known and assumed constant through time. The EOFs were obtained using a singular value decomposition (SVD) of a data matrix \mathbf{C} with columns

$$\underline{C}_i = \underline{c}_i - \bar{c}, \quad (2-3.1)$$

where \underline{c}_i are the real profiles available, and \bar{c} is the average profile. The SVD is known to be

$$\mathbf{C} = \mathbf{U}\mathbf{D}\mathbf{V}, \quad (2-3.2)$$

where \mathbf{D} is a diagonal matrix with the singular values, and \mathbf{U} is a matrix with orthogonal columns, which are used as the EOFs. The sound-speed profile is obtained by

$$\underline{C}_{EOF} = \bar{c} + \sum_{n=1}^N \alpha_n \underline{U}_n, \quad (2-3.3)$$

where N is the number of EOFs to be combined, judged to accurately represent the sound speed field for the problem at hand. Generally a criteria based on the total energy contained on the first N EOFs is used. Experimental results have shown that usually the 2 or 3 first EOFs are enough to achieve a high degree of accuracy. The use of EOFs

involves historical data that in the case of the water column sound speed profile can be acquired over time and space. Thus, one can expect to have sufficient information to enable the model to obtain a profile that best represents the watercolumn over range, depth and time. The 14 sound speed profiles obtained from the XBT measurements (see the TOMPACO data report [1]) served as database for the computation of the EOFs.

The criteria used to select the number of relevant EOFs for the available data was

$$\hat{N} = \min_N \left\{ \frac{\sum_{n=1}^N \lambda_n^2}{\sum_{m=1}^M \lambda_m^2} > 0.8 \right\} \quad (2-3.4)$$

where the λ_n are the singular values obtained by the SVD, M is the total number of singular values, provided that $\lambda_1 \geq \lambda_2 \geq \dots \geq \lambda_M$. For this data set criteria (2-3.4) yielded $N = 2$, i.e. the first two EOFs are sufficient to model the sound speed with enough accuracy (see figure 2.6). The coefficients α_n , which are the coefficients of the linear combination of EOFs, are now part of the search space, i.e., they are searched as free parameters.

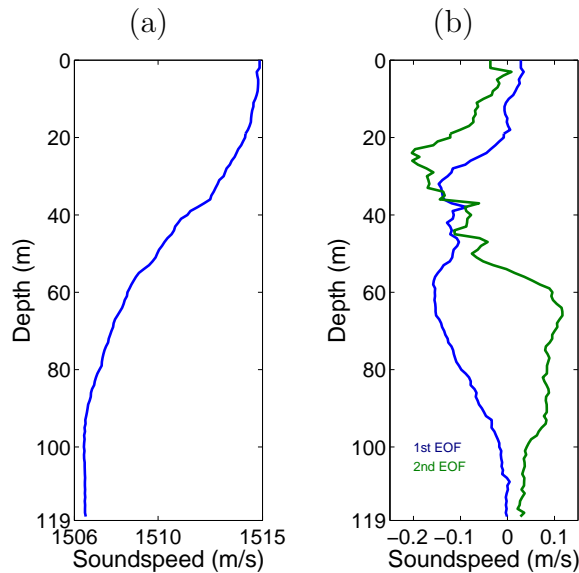


Figure 2.6: XBT based data used for ocean sound speed estimation: mean sound speed profile (a) and empirical orthonormal functions (EOFs) (b).

Chapter 3

The inverse problem

3.1 Focalization: a method for global inversion

Multiple environmental and geometrical parameter optimization is often a computationally cumbersome task. The optimization hypersurface may be very irregular leading to a severely ill-conditioned problem with a large number of local maxima. When dealing with real data, the inherent model mismatch and the presence of noise create a situation where there is no assurance of existence of an optimum solution in coincidence with (or even close) to the true model parameters. The first approach to the problem is to try to get as much apriori information as possible from the environmental parameters in the baseline model, in order to set them fixed and close to the true parameters so, the search is only done on a few unknown parameters. In practice, it is well known that setting fixed parameters in the model creates severe mismatches with real data that can not be overcome by the search parameters, leading to poor fit situations and strongly biased estimates. An alternative is a technique proposed by Collins et al. [7], known as focalization, where a number of a priori known model parameters, are allowed to be adjusted during the search process in order to compensate for the data-model misfit and possible measurement errors. Generally, a priori known parameters have a smaller degree of variation than the unknown parameters. This technique provides a high degree of fit and a better conditioned convergence to the true parameter values. Examples of such results are given in recent publications by the authors of this report [8, 9, 10, 11].

The second problem when inverting acoustic data are the difficulties associated with the representation of a time, depth and range variant field by a finite set of invariant parameters. This is the problem known as regularization, and has been dealt with in section 2.3, with a solution based on the expansion of the sound speed field (or equivalently the temperature field) on a set of depth dependent Empirical Orthogonal Functions. These EOF's were drawn from the observed data collected during the sea trial at various times and locations throughout the experimental site.

Finally, after a propagation model was selected, a canonical environmental scenario for focalization was built and a regularization technique was applied, we are ready to start the computation part, which is an important issue in ocean tomography. The optimization technique for reducing the number of forward computations was based on a genetic algorithm (GA).

3.2 GA Optimization

Principles of GA are now well known in the underwater acoustic community and different implementations have been widely used in practice with good results. GA parameter setting may have a strong influence on convergence to the solution and hence on the final result. These parameters have been set differently for each case and are explained below. The GA implementation used in this study was proposed by [12]. In particular, a new technique that was found to drastically optimize the search is to use the final solution at a given time point in the initialization of the solving procedure of the next time point.

Let us assume that at time t_i the best individual of the last population is $b(t_i)$. The GA is initialized at time t_{i+1} such that 30% of the individuals of the initial population are uniformly distributed within a 10% variation interval of the coordinates of $b(t_i)$. The other 70% are randomly distributed in whole search space as it is usually done, in order to maintain a high degree of diversity. With this procedure the number of iterations has been decreased at each time point except for the first one. In practice it is verified that the model fit drops at the beginning of each time point when compared with its value at the end of the previous time point, denoting that a misadjustment has been introduced in the data. However, after that initial fitness drop, rapid convergence is obtained leading to parameter values settling down to their "right" values, or at least those that give the highest fit. The objective function used in this study, was based on the incoherent Bartlett processor in a frequency band selected according to the sound source response function. The number and values of the selected frequencies varies with each case and as a general rule it was a compromise between the degree of difficulty of the problem at hand and the computational load.

3.3 Event II: moving source inversion in a range-independent environment

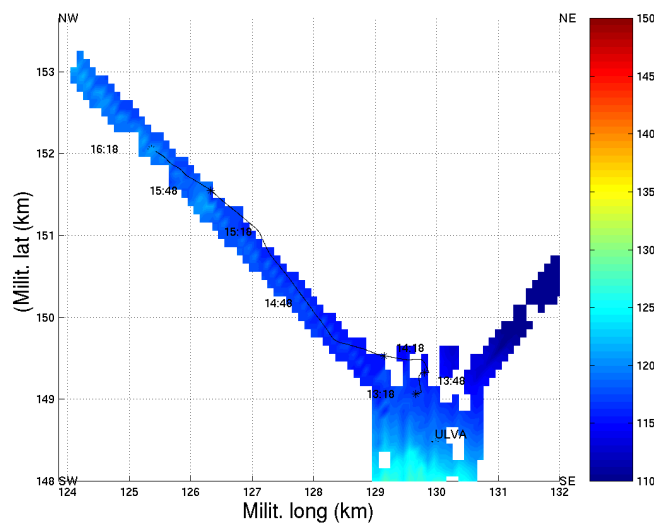


Figure 3.1: *Event II: bathymetry and ship course along NW leg.*

Event II took place along the range-independent NW leg from Oct 16, 14:48 to Oct 17,

14:15 local time. At the beginning of the run the source was moving away from the VLA location giving the opportunity to test forward and inverse methods with a moving source, which is known to be an always challenging exercise for matched-field algorithms. Source movement, as given by the onboard ship GPS is shown in figure 3.1 together with the bathymetry. The speed and heading of the ship towing the source, an important factor for result validation, is given in figure 3.2 and source range from the VLA estimated from GPS data is given in figure 3.3. The previously defined baseline model of figure was used as starting model in this inversion.

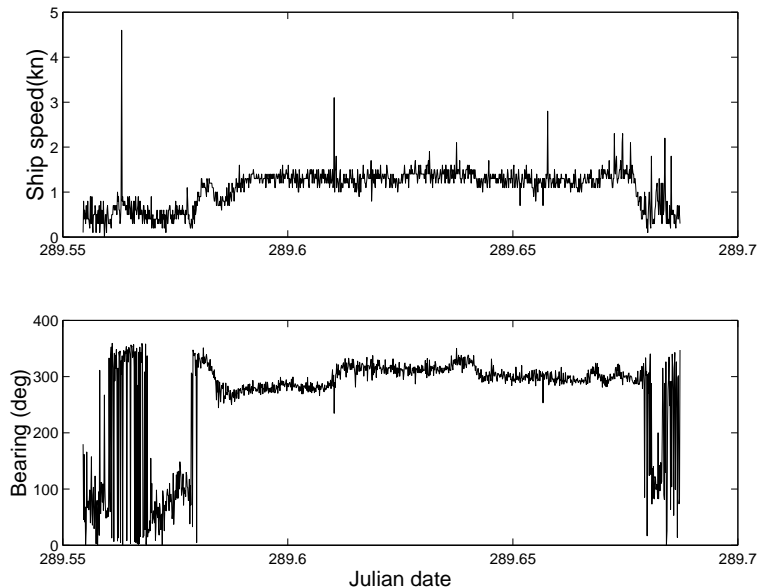


Figure 3.2: *Event II: source ship speed and heading along NW leg.*

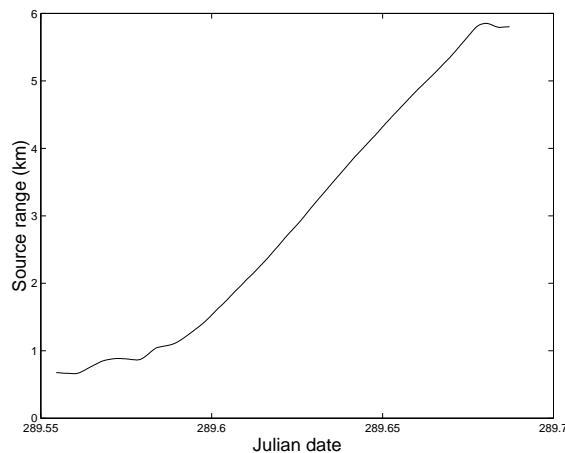


Figure 3.3: *Event II: source - VLA range as estimated from GPS data.*

The source was emitting a series of LFM signals which frequency range, duration and repetition rate is described in TOMPACO report [1], and is not repeated here since that information was neither explicitly or implicitly used in the present study in order to ensure passive tomography constraints. For each time point estimate three consecutive snapshots were averaged and Fourier transformed. From the resulting spectra 7 discrete frequencies 50 Hz apart in the band 300-600 Hz were extracted for computing the incoherent Bartlett processor.

In order to cover a search space of the order of 10^{15} , the GA optimizer was set with a population size of 90 individuals and 50 iterations. Three independent populations were run for each case. The mutation and the crossover probability were respectively set to 0.008 and 0.7. Table 3.1 lists the environmental and geometrical parameters included in the focalization process as well as their respective search intervals.

Table 3.1: *Event II: focalization parameters and search intervals. The subbottom compressional velocity is constrained to lay in the interval of the estimated sediment compressional velocity + 20 m/s and the upper bound of the sediment compressional velocity + 200 m/s.*

Parameter	Symbol	Unit	Search interval/Steps		
EOF 1	α_1	m/s	-20	20	64
EOF 2	α_2	m/s	-20	20	64
Source Range	sr	km	0.5	5.5	128
Source Depth	sd	m	10	100	64
Receiv. Depth	rd	m	85	95	32
VLA tilt	θ	rad	-0.03	0.045	32
Comp. speed sed.	c_{sed}	m/s	1520	1700	64
Sed. thickness	h_{sed}	m	1	15	32
Comp. speed bot.	c_{bot}	m/s	20	200	32

The results of the inversion are shown in figure 3.5. After focalization the sound speed evolution through time was constructed from the EOFs and the estimated coefficients of plots (i) and (j) of figure 3.5. Figure 3.4 gives on pannel (a) a time series of estimated sound speed profiles and on pannel (b) the depth-time plot of the inverted sound speed. Note that during this inversion the source was moving so the depth-time plot can also be seen as a depth-range plot, depending if the temperature field is assumed range stationary of time stationary, respectively.

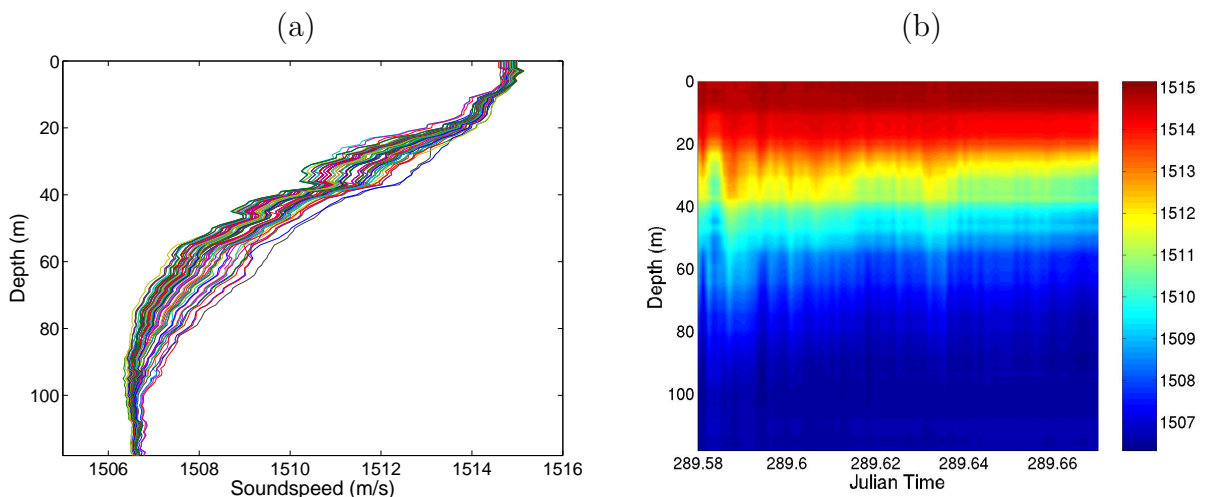


Figure 3.4: *Tomography results for ocean sound speed during moving source portion of Event 2: time series of sound speed profiles (a) and depth - time plot of inverted sound speed (b).*

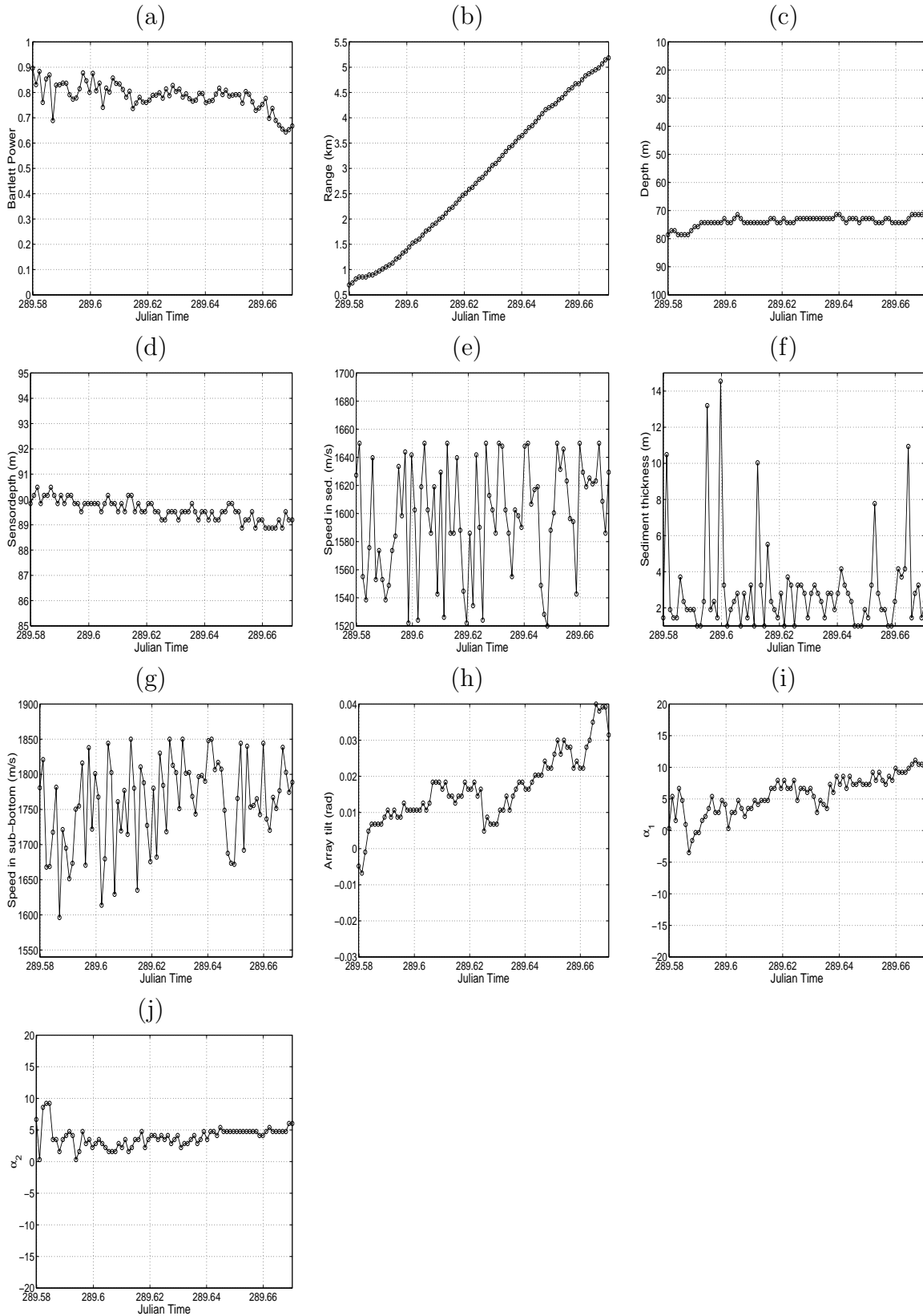


Figure 3.5: Focalization results for Event 2: Bartlett power (a), source range (b), source depth (c), receiver depth (d), sediment compressional speed (e), sediment thickness (f), sub-bottom compressional speed (g), VLA tilt (h), EOF coefficient 1 (i), EOF coefficient 2 (j).

These results call for the following comments: the first comment is that the model fit to the data is excellent with a mean Bartlett power of 0.8, only dropping below that value at the end of the run. Source range and depth are perfectly in agreement with the GPS estimated values (for the range). Note that even the small ship acceleration at the beginning of the run is perfectly reproduced with a consequent and logical decrease on the source depth from about 80 to 73 m. Receiver depth and tilt are consistent with the values monitored by the VLA sensors (see report [2]). Bottom properties are consistent with those historically found in that area that correspond to a thin (2 - 4 m) sediment layer of fine sand or mud.

There are two difficult, yet somehow separated tasks, when attempting to match model and reality: one is to capture time (or frequency) variation of the received signal and the other is to be able to represent spatial dependence of the received field. The time response obtained at selected locations and for some hydrophones has been shown in [13]. For the spatial dependence the problem is complicated by the fact that such representation is to be made along depth through the VLA and along range since the source is moving and range is varying continuously with time. As an example, figure 3.6 shows the comparison of the measured acoustic field at the VLA, with that simulated using CSNAP with the baseline environmental model of figure 2.5 and that obtained with the same CSNAP but after environment focalization.

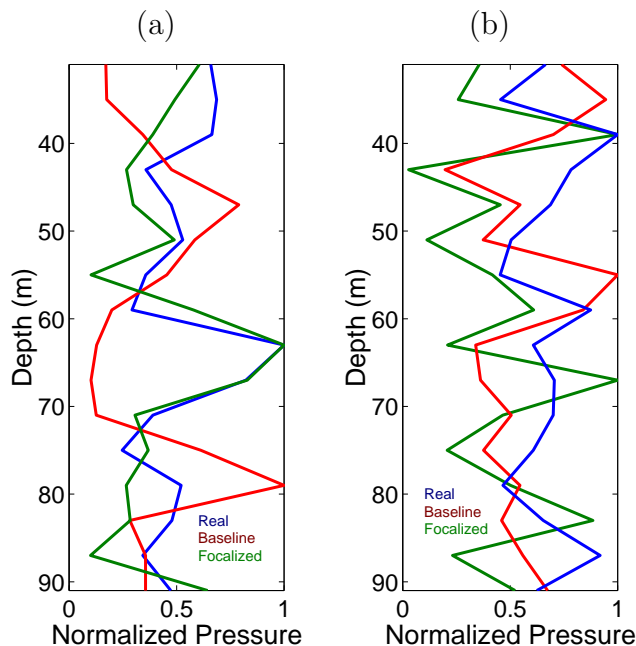


Figure 3.6: Comparison of the VLA received acoustic pressure with the CSNAP prediction using the baseline model and the model after focalization at frequencies of: 300 Hz (a) and 500 Hz (b).

3.4 Event V - range independent, PRN stationary source

This case is drawn from Event V, that was specifically designed for TOMPACO, where the sound source was emitting a pseudo random noise (PRN) sequence and making an

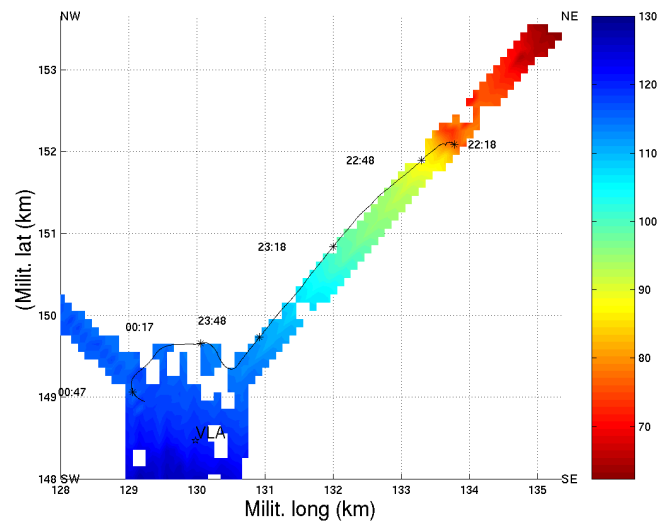


Figure 3.7: *Event V: bathymetry and ship course along NE leg.*

arc shaped movement around the VLA in an assumed range-independent environment. The source-receiver geometry for that event is shown in figure 3.7 and the corresponding ship speed and course is shown in figure 3.8 for Julian date after 291. For the same time interval the source-receiver range as estimated from the GPS data is shown in figure 3.9. The assumed model is the baseline model shown in figure 2.5 and used for Event 2.

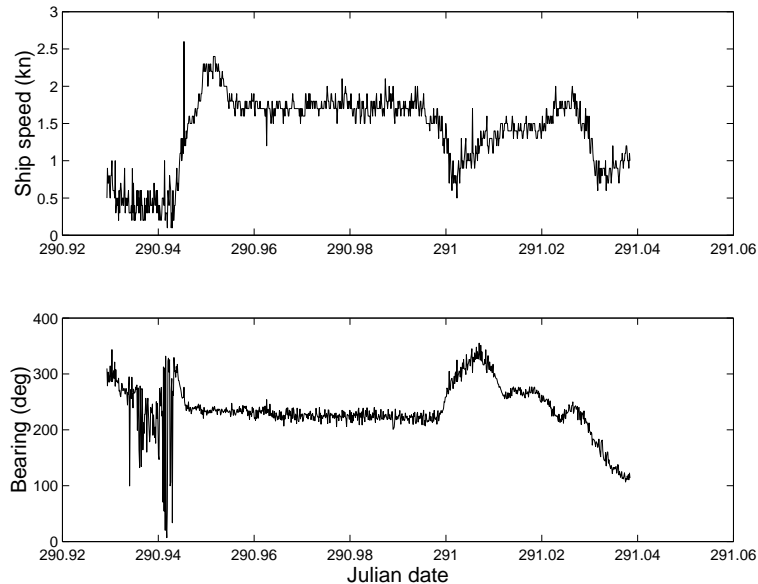


Figure 3.8: *Event V: source ship speed and heading along NE leg.*

Since the processor is based on a incoherent sum across frequency, the PRN signal should provide a similar performance than that of the LFM's of Event 2. The estimation of the spectral density matrices is made from an average of 16 Fourier transformed vectors of 2 s of data each, for 13 frequencies spaced 25 Hz in the band 300-600 Hz. Search parameters, GA initialization and baseline model are identical to those for Event 2. The results of the inversion are shown in figure 3.11.

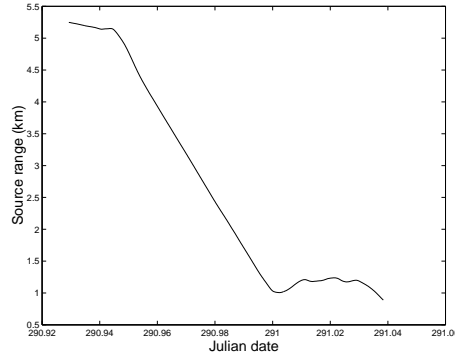


Figure 3.9: *Event V: source - VLA range as estimated from GPS data.*

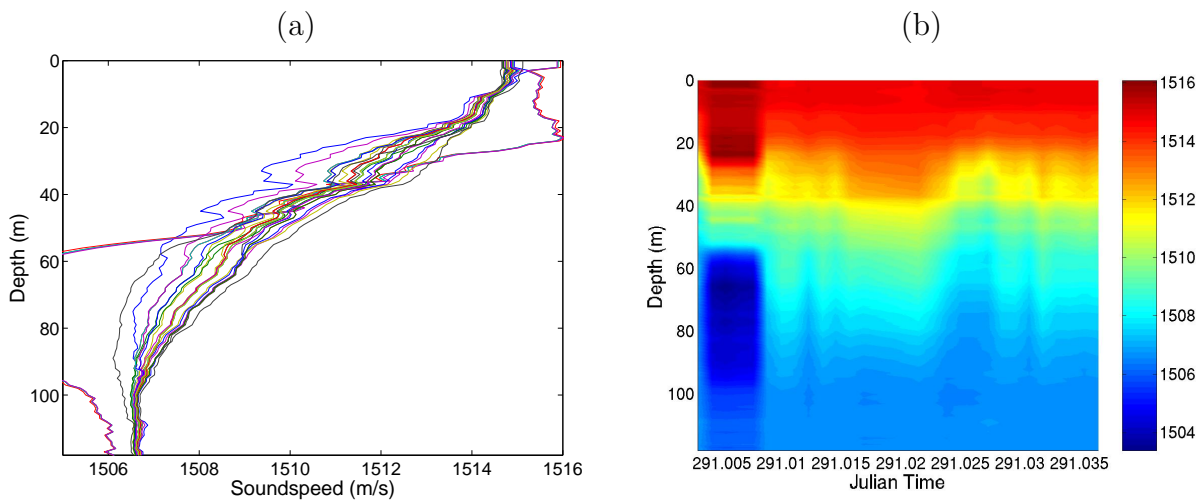


Figure 3.10: *Tomography results for ocean sound speed during arc shaped moving source portion of Event 5: time series of sound speed profiles (a) and depth - time plot of inverted sound speed (b).*

After focalization the sound speed evolution through time was constructed from the EOFs and the estimated coefficients of plots (i) and (j) of figure 3.11. Figure 3.10 gives on pannel (a) a time series of estimated sound speed profiles and on pannel (b) the depth-time plot of the inverted sound speed. Note that also during this run the source was moving along an arch so the depth-time plot can also be seen as a depth-bearing plot, depending if the temperature field is assumed space stationary or time stationary, respectively.

From these results, the following comments can be made: the Bartlett power has a larger variation than in the previous Event with starting values that denote a complete misfit in the first minutes of the data set and then raising to values around 0.8 providing a good indicator of correct data inversion. At the end of the run the source was shutoff so there is a clear Bartlett power drop. Values at the beginning and at the end of the run should be disregarded for the inversion. Source position is consistent with the GPS data for range and depth recordings show that during that part of the experiment the source was much shallower¹. Receiver depth and tilt need no comments. Bottom properties are very difficult to estimate at this source range with such small bottom interaction. EOF coefficients have a consistent evolution that is not very significant since the total

¹this was due to the fact that Event 5 covered a shallower area with water depths reaching 60 m thus the sound source was raised for precaution to avoid hitting the bottom.

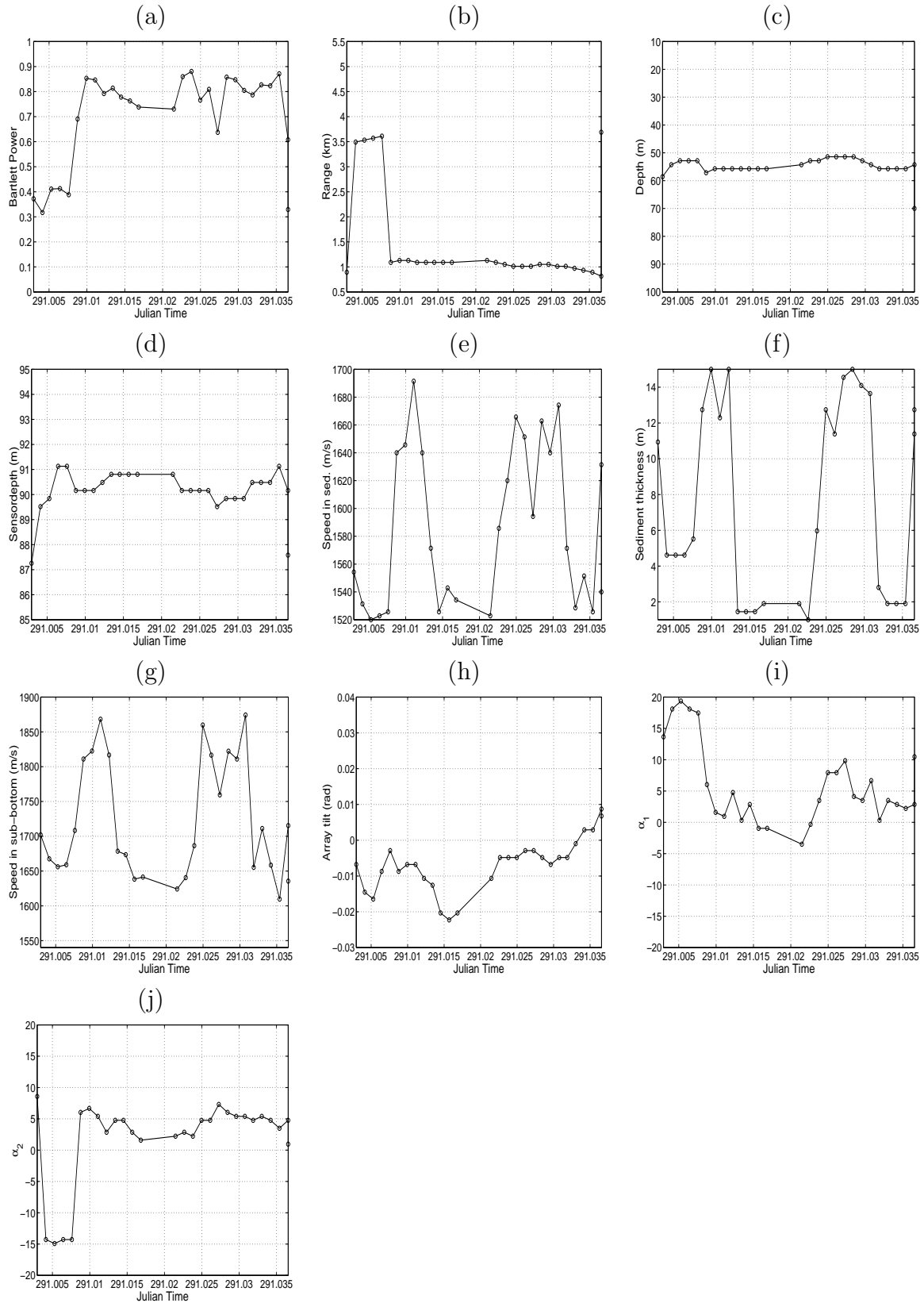


Figure 3.11: Focalization results for arc shaped portion of Event 5: Bartlett power (a), source range (b), source depth (c), receiver depth (d), sediment compressional speed (e), sediment thickness (f), sub-bottom compressional speed (g), VLA tilt (h), EOF coefficient 1 (i), EOF coefficient 2 (j).

duration of the run is only about 90 min.

3.5 Event V - range dependent, PRN moving source

Although a range-independent propagation environment is a view of the reality that allows nice theoretical analytical developments, it is, in most cases only a simplified view that does not represent the large majority of the real world situations. When operating in coastal waters, the typical environment consists of a sloping bottom from the deep ocean to the continental platform. In real world passive tomography applications the sound sources (ships of opportunity) are generally located on the deeper side and emitting to a receiver located on the shallower side: that is upslope propagation. Due to the acoustic reciprocity principle, interchanging source and receiver would lead to the same received acoustic field so there is absolutely no loss of generality when studying the downslope case, as it was done during the INTIFANTE'00 experiment in Event IV and V.

In this section the data gathered during Event V, along the NE leg, when the source was at about 5 km range and then approaching the receiver is used to downslope propagate from approximately 70 m water depth to the VLA located in 120 m water depth (see figure 3.7). The baseline environmental model of figure 2.2 was used to produce a range dependent model to represent the downslope propagation of this portion of the event. Only the bathymetry was changed. Geoacoustic parameters and water sound speed profile were kept unchanged as it can be seen in figure 3.12.

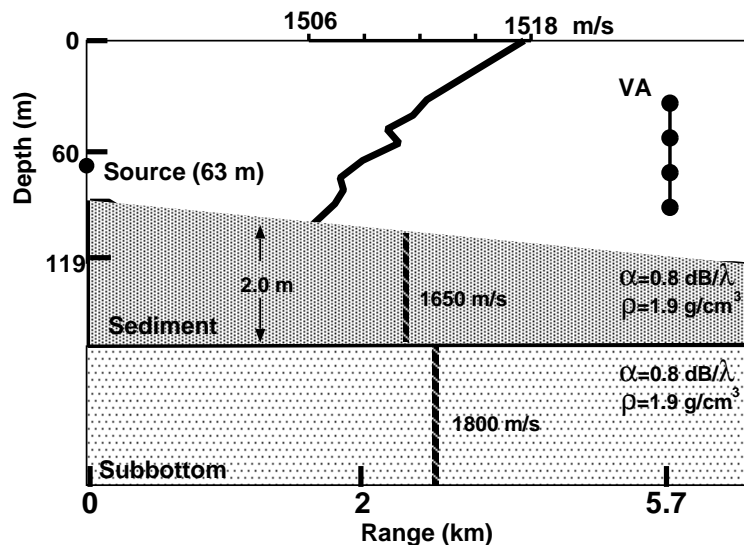


Figure 3.12: *Baseline environmental model for the range-dependent propagation scenario of Event 5.*

This is the most interesting yet most difficult case that attempts to represent a realistic situation of an unknown sound source emitting a PRN sequence at an undetermined range and depth moving over a range dependent environment. The results of the inversion are shown in figure 3.14.

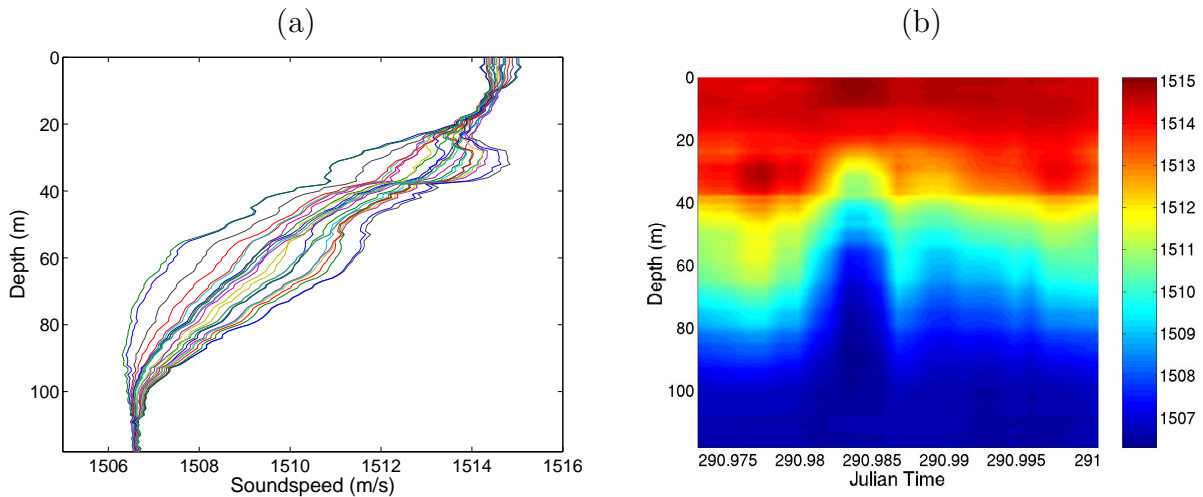


Figure 3.13: *Tomography results for ocean sound speed during range-dependent moving source portion of Event 5: time series of sound speed profiles (a) and depth - time plot of inverted sound speed (b).*

After focalization the sound speed evolution through time was constructed from the EOFs and the estimated coefficients of plots (i) and (j) of figure 3.14. Figure 3.13 gives on pannel (a) a time series of the estimated sound speed profiles and on pannel (b) the depth-time plot of the inverted sound speed. This a short duration run of only about 60 min which is not very significant in terms of sound speed evolution. The Bartlett power has a remarkably stable value at high values with an increasing trend when the source approaches the VLA. Source position is also remarkably stable at 50 m depth (which is in agreement with a stable source speed as seen in 3.8), while the source ship is navigating from a shallower area, and decreasing range with a good match with the GPS measured range of figure 3.9. Receiver depth is stable at correct values, and array tilt tends to the lower limit of the search space, so that bound, that represents a array top deviation of approximately 2.5 m, needs to be enlarged in future search with this data. Bottom properties call for the same comment as previously but show consistent values. As a general trend shown by geophysical property charts of thea area, the source is navigating over a zone with bottom variability, passing from clay to sand and with a probable variation of sediment thickness. More environmental data evidence should be provided by Instituto Hidrográfico ² to validate these results. EOF coefficients have a consistent evolution with a strong trend at the middle of the run for the first coefficient α_1 . There is no independent information to validate this result.

²side scan and Uniboom data analysis has been terminated at Instituto Hidrográfico and a report is being written at this time.

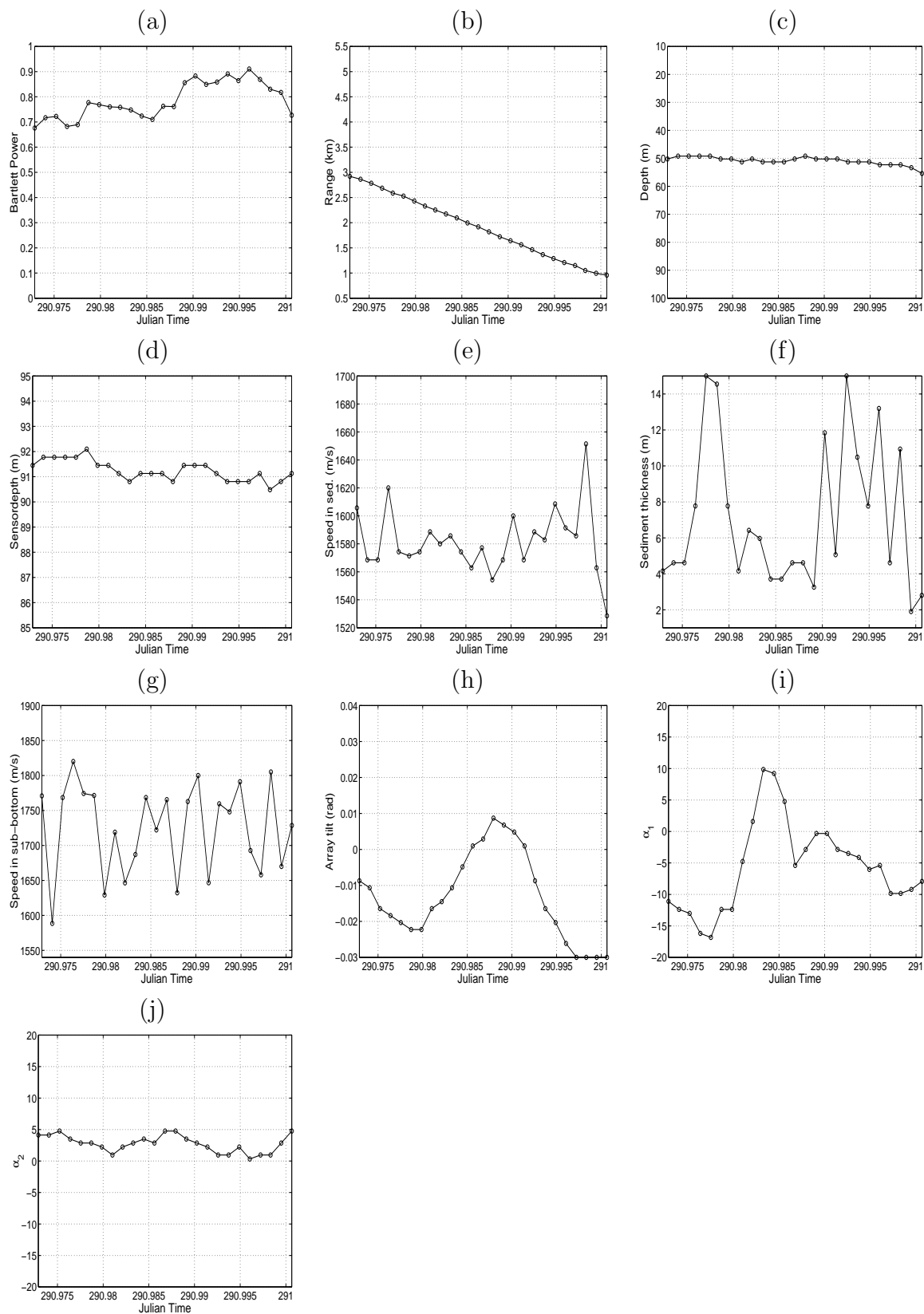


Figure 3.14: Focalization results for range-dependent portion of Event 5: Bartlett power (a), source range (b), source depth (c), receiver depth (d), sediment compressional speed (e), sediment thickness (f), sub-bottom compressional speed (g), VLA tilt (h), EOF coefficient 1 (i), EOF coefficient 2 (j).

Chapter 4

Conclusion

OAT is an appealing technique for remote monitoring of the ocean volume. One of the basic principles of OAT is that both source(s) and receiver(s) are under control of the experimentalist - that is the emitted source signal and the source-receiver geometry is known (with some degree of precision) at all times during the observation window. In passive tomography the control of the source is relaxed in order to be able to take advantage of possible sources of opportunity passing within acoustic range from the receiver(s). Although passive tomography is very appealing for the ease of application, its practical implementation is extremely challenging and its feasibility remains to be proved.

This study reports the tomographic inversion results obtained on part of the data obtained during the INTIFANTE'00 sea trial aiming at proving the feasibility of passive tomography in a first attempt with an towed sound source emitting noise sequences. The challenge is represented by the fact that during the various phases of the processing the a priori knowledge about the source is progressively relaxed leading to a situation close to that encountered in passive tomography.

In a first data set it was proved that a moving source at an unknown location emitting a deterministic unknown signal over a range-independent environment can be used for ocean tomography when the environment is progressively adapted through time. Estimates of the various environmental and geometrical parameters are consistent with expected values. Focalization was proved to represent the tool of choice for accounting for the unknown geometrical and environmental parameters, inherent to passive tomography feasibility.

In a second data set a moving source at an unknown location was emitting an (assumed) unknown PRN sequence and its signals were used for determining the sound speed structure as well as other geometrical and geoacoustic parameters. The results showed also to be consistent with the expectations and demonstrated that the employed methods can operate with pseudorandom noise source signals.

Finally, in a third data set, the same source was moving towards the array emitting a PRN signal over a range-dependent environment, representing a scenario close to the real passive tomography scenario. It was shown that also in this close to real scenario, both geometrical and environmental parameters were consistently estimated over time resulting in a high model fit indicating a potential for accurate inversion estimates.

In terms of future work there is a need for completing the processing of these runs of Event 2 and 5. It would also be interesting to invert the acoustic data of Event 4 and compare geoacoustic environmental results of the same area, between Event 4 and

Event 5, while the signals being transmitted are deterministic LFM's and PRN sequences, respectively. The processing of the 24 hours long results of Event 2 would allow for a more accurate picture of the inverted temperature data. Finally, the inversion of the ship noise data during Event 6 would provide the last demonstration of feasibility of the methods being developed. At this point of the study, with the consistent results obtained so far, there is almost certainty that an inversion is at reach with ship noise data during this experiment. Additionally, the results should be completed by a statistical study aiming at providing a confidence bound on each final estimate. As an experimental side comment, more attention should be given in future experiments to acquire independent data, both sea bottom properties and water column time and space variation, in order to be able to validate the data being inverted with acoustic measurements.

Bibliography

- [1] Jesus S. Tomografia passiva costiera, data report - phase 1. Internal Report Rep. 01/01, SiPLAB/CINTAL, Universidade do Algarve, Faro, Portugal, March 2001.
- [2] Jesus S., Silva A., and Soares C. Intifante'00 sea trial data report - events i, ii and iii. Internal Report Rep. 02/01, SiPLAB/CINTAL, Universidade do Algarve, Faro, Portugal, May 2001.
- [3] C. M. Ferla, M. B. Porter, and F. B. Jensen. *C-SNAP: Coupled SACLANTCEN normal mode propagation loss model*. La Spezia, Italy.
- [4] Collins M.D. *Users's Guide for RAM Versions 1.0 and 1.0p*. Washington DC, USA.
- [5] Rodríguez O.C., Jesus S., Stephan Y., Démoulin X., Porter M., and Coelho E. Internal tide acoustic tomography: reliability of the normal modes expansion as a possible basis for solving the inverse problem. In *Proc. of the 4th. European Conference on Underwater Acoustics*, pages 587–592, Rome, Italy, 21-25 September 1998.
- [6] Rodríguez O.C. Hydrodynamical normal mode estimation on the intifante'00 data set. Internal Report Rep. 04/01, SiPLAB/CINTAL, Universidade do Algarve, Faro, Portugal, November 2001.
- [7] Collins M.D. and Kuperman W.A. Focalization: Environmental focusing and source localization. *J. Acoust. Soc. America*, 90(3):1410–1422, September 1991.
- [8] Soares C., Waldhorst A., and Jesus S. Matched field processing: Environmental focusing and source tracking with application to the north elba data set. In *Proc. of the Oceans'99 MTS/IEEE conference*, pages 1598–1602, Seattle, Washington, 13-16 September 1999.
- [9] Soares C.J., Siderius M., and Jesus S.M. Matched-field source localization in the strait of sicily. *submitted to J. Acoust. Soc. America*, July 2001.
- [10] Soares C., Siderius M., and Jesus S. Mfp source localization in the strait of sicily. In *Proc. of the MTS/IEEE Oceans 2001*, Honolulu, Hawaii, USA, 5-8 November 2001.
- [11] Soares C.J. and Jesus S.M. Broadband matched-field processing: coherent vs. incoherent approaches. *submitted to J. Acoust. Soc. America*, December 2001.
- [12] T. Fassbender. *Erweiterte genetische algorithmen zur globalen optimierung multimodaler funktionen*. Diplomarbeit, Ruhr-Universität Bochum, 1995.
- [13] Jesus S., Coelho E., Onofre J, Picco P, Soares C., and Lopes C. The intifante'00 sea trial: preliminary source localization and ocean tomography data analysis. In *Proc. of the MTS/IEEE Oceans 2001*, Honolulu, Hawaii, USA, 5-8 November 2001.